e-Navi

Available online at http://www.e-navigation.kr/
e-Navigation Journal

Original article

A study of the effect of deflector outlet inlet angle on the energy acquisition efficiency of hydraulic turbine

Zekai SUN[a] , Guang SUN[b], Haihua LIN[c]

[a] Naval Architecture and Port Engineering College, Shandong Jiao Tong University, Weihai 264209, China, 1486497129@qq.com

[b] Naval Navigation and shipping College, Shandong Jiao Tong University, Weihai 264209, China, 220152@ sdjtu.edu.cn

[C] Naval Architecture and Port Engineering College, Shandong Jiao Tong University, Weihai 264209, China, 222018@sdjtu.edu.cn

Abstract

Hydraulic turbines can convert tidal current energy into electric energy, and the addition of a deflector cover to the turbine can improve the efficiency of the turbine's energy harvesting. The angle of the inlet section and the angle of the outlet section of the deflector will further affect the final energy-acquisition efficiency.A three-dimensional numerical model for turbine flow field analysis is established, and the RNG k-ε turbulence model is selected by CFD method, and the best angles of inlet section and outlet section are analysed by the method of sliding mesh to obtain the best angle of inlet section and outlet section separately, and then three groups of angles are selected near the best angle of inlet section and outlet section to make orthogonal comparisons. The energy acquisition efficiency of the turbine is calculated at different angles of the inlet and outlet sections of the deflector, and the turbine streamline distribution, velocity and pressure maps are analysed with and without the deflector.The study shows that the deflector can play the role of convergence of the downstream flow, which can improve the efficiency of the turbine energy acquisition, and the maximum energy acquisition efficiency is at the inlet angle of 29° and the outlet angle of 40 °, and the maximum energy acquisition efficiency can be improved by about 32 percent.

Keywords: Deflector, energy capture efficiency, inlet section angle;, outlet section angle

https://doi.org/10.52820/j.enavi.2024.22.001

1. Introduction

Energy is an important material basis for economic development, and human development cannot be separated from the use of high-quality energy and advanced energy technology. With the development of the world economy, human demand for energy is growing (2016, p.12). In recent years, with the depletion of traditional fossil energy sources and the increasing deterioration of the environment(2019, p.12)the sustainable development of global energy has become a common challenge for all countries in the world(2017, p.12). As a kind of green renewable energy in the ocean, tidal current energy has the advantages of wide distribution, large energy and stability(2009, p.12-LUND H, 2007). Water turbine As the core component of the energy captured by the tidal current energy generator, the energy acquisition efficiency of the machine is a hot research topic in the field of sea current energy generation (2013, p.12). In order to improve the power generation efficiency of the tidal current energy turbine, the commonly adopted method is to add a current-concentrating device, i.e., a deflector cover, to the periphery of the impeller. The turbine with a deflector can allow more fluid to pass through the rotating plane of the rotor, which can increase the flow velocity and stabilise the flow field, thus effectively improving the utilisation efficiency of the ocean current energy (2022, p.12).

Scholars have studied the hydrodynamic performance of the hydraulic turbine after the addition of the deflector cover from different angles. Lan Yamei et al (2020, p.12) selected three factors, namely, the angle of the inlet section of the deflector hood, the angle of the outlet section and the spacing, to make a comparative analysis of the efficiency of the transverse-axis hydraulic turbine in terms of energy gain, and obtained that the magnitude of the influence of the energy utilisation rate of the transverse-axis turbine was in the following order: the angle of the inlet section of the deflector hood > the spacing > the angle of the outlet section.Wang Shujie et al. (2022, p.12).investigated hydrodynamic performance of the deflector hood with the length of flare section of 250mm, 350mm and 450mm respectively when the inlet section is 15°, and got the best hydrodynamic performance of the deflector hood at 450mm.SONG et al. (2019, p.12).selected the deflector hoods with the inlet section of 6°, 12°, 18° and 24°, and found that the efficiency of the turbine's energy acquisition showed a trend of increasing firstly and then decreasing.

Up to now, most of the studies by scholars tend to explore the angle of the inlet and outlet sections as fixed values. So far, there has not been any study to obtain the optimal angles of the inflow and outflow sections of the deflector by comparing the energy acquisition efficiency of the hydraulic turbine. Therefore, it is necessary to carry out further related studies to reveal more comprehensively the influence mechanism of the angle of the inlet and outlet sections on the hydrodynamic performance of the deflector hood. In this paper, the hydrodynamic performance of the hydraulic turbine deflector hood is analysed based on the CFD method at different angles of the inlet and outlet sections, so that the optimal angles of the inlet and outlet sections associated with the maximum energy-acquisition efficiency are determined.

2. Numerical method

2.1 control equations

Let the fluid around the turbine be an unpressurised Newtonian fluid, which satisfies the continuity equation, i.e., the law of conservation of mass (2012, p.12). and its fundamental governing equation is:

$$\frac{\partial \rho}{\partial t}+\frac{\partial(\rho u_i)}{\partial x_i}=0 \qquad (1)$$

$$\frac{\partial(\rho u_i)}{\partial t}+\frac{\partial(\rho u_i u_j)}{\partial x_j}=-\frac{\partial p}{\partial x_i}+\frac{\partial}{\partial x_i}(\mu\frac{\partial u_i}{\partial x_j}-\rho\overline{u_i' u_j'})+S_j \qquad (2)$$

where:

ρ is current density;

u_i is the velocity component corresponding to the point;

P is pressure at a point in space at time t;

μ is fluid power viscosity coefficient;

$\rho\overline{u_i' u_j'}$ is reynolds stress term;

Sj is adding source items;

2.2 Turbulence model

Under the action of turbulence, the water flow passing through the impeller will produce rotation. Compared with the same general turbulence pattern, the rotational

effect will cause the near-wall pulsating rotation, and the intensity of circumferential turbulence will be further enhanced (2005, p.12)and the rotation generates turbulence with prominent radiation characteristics in all directions, which is more likely to flow separation (Wang Shijun, 2016).The RNG k-ε turbulence model can better simulate the complex state of the fluid impact, separation and rotation, so this paper adopts this model for analysis, and its mathematical model is as follows

$$\rho\frac{Dk}{Dt}=\frac{\partial}{\partial x_i}\left[\left(\mu+\frac{\mu_t}{\sigma_k}\right)\frac{\partial k}{\partial x_i}\right]+G_k-\rho\varepsilon \qquad (3)$$

$$\rho\frac{D\varepsilon}{Dt}=\frac{\partial}{\partial x_i}[(\mu+\frac{\mu_t}{\sigma_\varepsilon})\frac{\partial\varepsilon}{\partial x_i}]+C_{\varepsilon1}\frac{\varepsilon}{k}G_k-C_{\varepsilon2}^{*}\rho\frac{\varepsilon^2}{k} \qquad (4)$$

$$C_{\varepsilon2}^{*}=C_{\varepsilon2}+\frac{C_\mu\eta^3(1-\eta/\eta_0)}{1+\beta\eta^3} \qquad (5)$$

where:

G_k is turbulent kinetic energy k generating term;

μ_t is viscosity coefficient of turbulent eddy masses;

σ_k is a constant math(0.72);

σ_ε is a constant math(0.75);

$C_{\varepsilon1}$ is a constant math(1.42);

$C_{\varepsilon2}$ is a constant math(1.68);

C_μ is a constant math(0.0845);

2.3 Energy efficiency

The energy acquisition efficiency of the turbine in the sea current is the efficiency of the turbine in acquiring mechanical energy from seawater, i.e. the ratio of the mechanical output power of the turbine to the input current energy. Denoting the energy acquisition efficiency by *Cp*

$$C_P=\frac{P}{\frac{1}{2}\rho v^3\pi R^2} \qquad (6)$$

where:

v is incoming flow rate;

R is radius of turbine;

$$P=\frac{1}{2}J\omega^2 \qquad (7)$$

where:

J is moment of inertia of the turbine about its own axis of rotation;

ω is angular velocity of rotation of the turbine;

3. Computational model

3.1 Computational models

In order to study the effect of different angles of attack of the inlet and outlet sections of the deflector on the hydrodynamic performance of the turbine, the 3D model of the turbine is built first. The NACA airfoil is relatively simple in structure, has a high lift-to-drag ratio, and has abundant data, so it is also used in turbine blades nowadays. Because NACA4415 has better pitch balance and smooth change of lift-to-drag ratio in NACA44XX series(Luo Ruidong 2020).this paper adopts NACA4415 airfoil to construct the hydraulic turbine blade, and the rotor radius R of the hydraulic turbine is 1000mm, and its basic parameters are shown in Table 1.

Tab. 1 Basic Blade Parameters

r/R	*c/R*	*θ/* (°)
0.2	0.092	5.1
0.3	0.094	6.4
0.4	0.102	8.2
0.5	0.111	10.6
0.6	0.120	13.5
0.7	0.130	17.0
0.8	0.140	21.1
0.9	0.152	24.2
1.0	0.156	29.2

In Table 1, *r/R* is the relative position of the airfoil blade section, *c* is the airfoil chord length, *c/R* denotes the relative width of the airfoil blade section profile at that position, and θ is the torsion angle. The torsion angle is the angle between the chord of the airfoil section and the plane of rotation perpendicular to the horizontal axis of the turbine (2007, p.12). Based on the above data, the models of the blade and the turbine obtained are shown in Fig. 1 and Fig. 2, respectively.

Fig. 1 Blade model

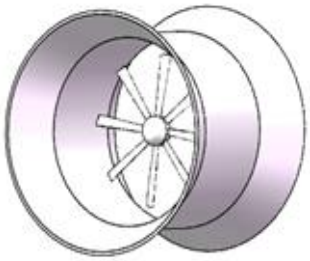

Fig. 2 Hydraulic turbine model

Figure 3 shows the side view section of the turbine, and the basic parameters of the turbine external de flector are shown in Table 2.

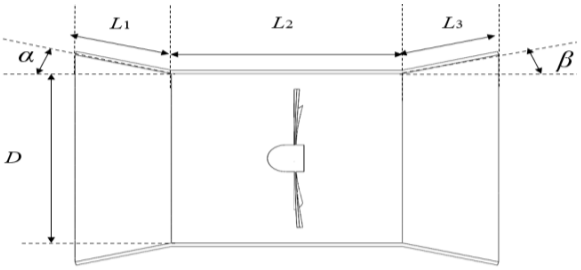

Fig. 3 Side view profile of the deflector shield

Tab. 2 Basic parameters of the deflector shield

inside diameter D /(mm)	2400
Entrance length L_1/(mm）	1100
Intermediate length L_2/(mm）	2400
Outlet length L_3/(mm）	1100
Entrance angle α/(°）	0-70
exit angle β/(°）	0-70

3.2 Flow filed region and boundary conditons

Denoting the turbine rotor diameter by D, the length of the flow field is 30D, the width and height are both 10D, and the set turbine centre position is 6D from the inlet and 24D from the outlet to establish the basin. The fluid domain inlet boundary condition is set as velocity inlet, the outlet boundary is set as pressure outlet, and the outer surface is set as intersection interface. The fluid domain and rotating domain interfaces are set as intersecting interfaces for data exchange, and the blades as well as the deflector shield portion are set as no-slip wall surfaces. (2006, p.12). shown in Figure 4

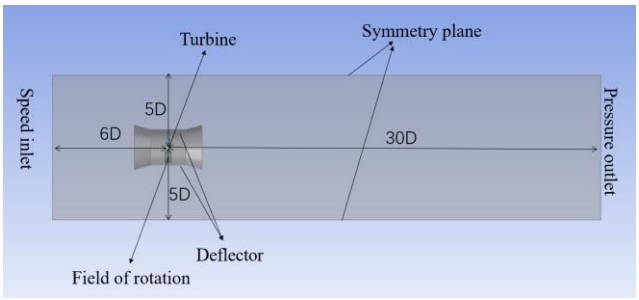

Fig.4 Boundary conditions and catchment modelling

3.3 Irrelevance verification

The grid-independence of the turbine model was verified, and the results of the energy acquisition efficiency calculations are shown in Table 4.

serial number	Grids	Rotated domain grid size	energy efficiency *Cp*
1	969628	130	9.55%
2	1771504	100	10.26%
3	2832275	70	10.85%
4	3671504	40	11.15%
5	4459934	10	11.15%

3.4 Grid plot

In the near-wall treatment, 6 layers of boundary layers are set, and the mesh height of the first layer corresponds to $y^+\approx1$. Soft behavior is selected for grid size growth to make sure that the generated mesh is more tightly connected and the growth rate is set to 1.03. The grid is shown in Figure 5.

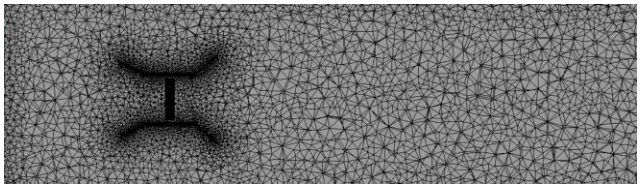

Figure 5: Grid Plot

4. Analysis conditions

The calculated working conditions are divided into β is 0° and α changes; α is 0° and β changes, as sh own in Table 5.

Tab. 5 Calculation condition

β be 0° and α change	α be 0° and β vary
10°, 15°, 20°, 25°, 27°, 28°, 29°, 30°, 35°, 40°, 50°, 60°, 70°	10°, 15°, 20°, 25°, 30°, 35°, 39°, 40°, 41°, 50°, 60°, 70°

According to the calculation results, suitable α and β were selected to carry out orthogonal experiments, as shown in Table 5.

Tab. 5 Orthogonal programme

serial number	A11	A12	A13	A21	A22	A23	A31	A32	A33
α	27°	27°	27°	28°	28°	28°	29°	29°	29°
β	39°	40°	41°	39°	40°	41°	39°	40°	41°

5. Analysis results

5.1 Energy efficiency results

The turbine flow field is analyzed according to the aforementioned method to obtain the turbine energy acquisition efficiency for each operating condition, as shown in Fig. 6.

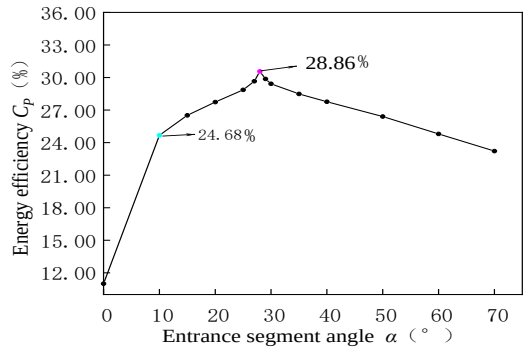

Deflector shield inlet section angle

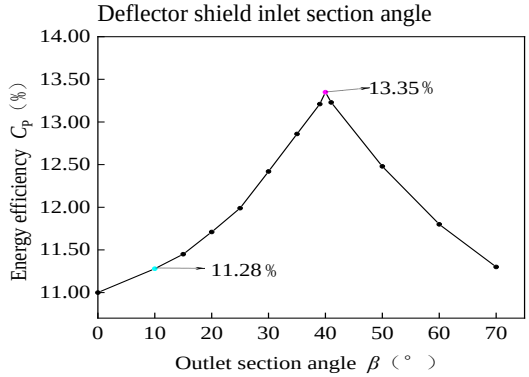

Deflector shield outlet section angle

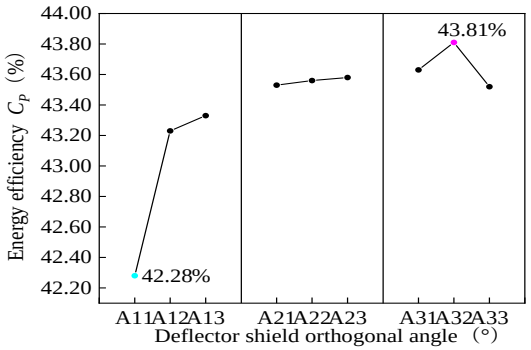

(3) Deflector angle orthogonal scheme

Fig. 6 Results of hydraulic turbine energy efficiency un der different flare angle

As can be seen in Figure 6:

(1) When α = 0° and β = 0°, the energy acquisition efficiency Cp of the turbine is the smallest, which is 11.15%; β is unchanged, and with the increase of α, the Cp of the turbine increases rapidly, and when α = 10°, the Cp = 24.68%; then, with the increase of α, the Cp increases slowly, and when α = 29°, the Cp reaches the maximum, which is 28.86%; and after the α continues to increase, the Cp begins to decrease.

(2) α is unchanged, as β increases, the energy acquisition efficiency Cp of the hydraulic turbine increases, but the increase is relatively slow compared with that of changing the inlet angle, when β=10°, Cp=11.28%; then, as β increases, Cp increases faster, and Cp reaches the maximum of 13.35% when β=40°, but it is smaller than that of the maximum of 28.86% obtained by changing the inlet angle; when β continues to increase, Cp starts to decrease. increase, Cp then starts to decrease.

(3) After the orthogonal optimization of the angles of the inlet and outlet sections, the turbine energy-acquisition efficiency obtained is better than that of only α-angle change or only β-angle change, and the turbine energy-acquisition efficiency Cp is the smallest when α=34° and β=39° within the range of orthogonal angles, which is 42.28%; and the turbine energy-acquisition efficiency Cp is the largest when α=29° and β=40°, which is 43.81%.

5.2 Flow field analysis

In order to analyse the mechanism of improving the energy-acquisition efficiency of the hydraulic turbine by the deflector, the A32 condition with the highest energy-acquisition efficiency of the deflector is compared with the flow field of the hydraulic turbine when the angles of the inlet and outlet sections are zero (equivalent to the

absence of the deflector). Fig. 7 shows the velocity cloud diagrams of the turbine without and with the deflector.

(1) The flow velocities inside the deflector are different, and overall, along the direction of incoming flow, the flow velocity at the turbine is greater than that at the inlet section; the velocity at the turbine paddle shaft is less than that near the blades and greater than that at the inlet; Maximum flow velocities in the vicinity of the turbine can be up to 1.2 times the incoming velocity.

(2) When there is no deflector, the maximum velocity is located in front of the turbine, and the flow velocity in a larger area near the turbine is smaller than the incoming flow velocity, and a larger area of low velocity zone is formed behind it; when the deflector is installed, the flow velocity in the inside of the deflector and in the vicinity of the turbine is greater than the incoming flow velocity, and the corresponding range is larger. It can be seen that the velocity gradient of the flow field around the turbine increases after the installation of the deflector cover, and the efficiency of energy acquisition is improved.

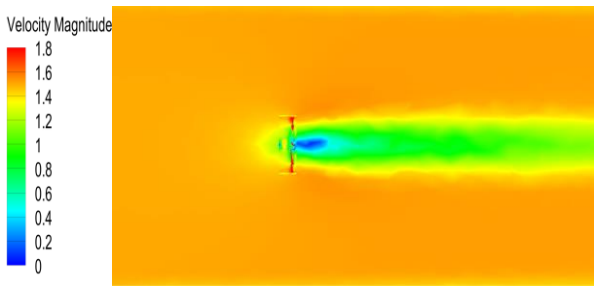

α=0°，β=0°

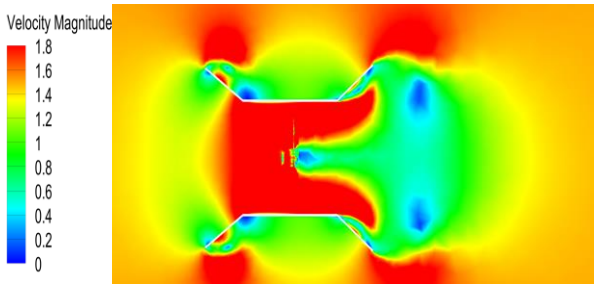

α=29°，β=40°

Fig. 7 Velocity cloud diagram

Fig. 8 shows the pressure cloud of the turbine without and with deflector, from the comparison of Fig. 7 it can be seen that

(1) A large pressure gradient is generated in the inlet section of the deflector, which is due to the fact that when the sea current flows through the deflector, the incoming velocity is reduced due to the obstruction of the structural surface of the inlet section, and a high-pressure region is generated in the inlet section to form a pressure difference with the low-pressure region of the intermediate section, which makes the angular velocity of the turbine accelerate, and thus increases the energy-acquisition efficiency of the turbine.

(2) The high-pressure area is mainly distributed in the inlet section, and with the increase of opening angle, the area of high-pressure area in the inlet section gradually increases, and the low-pressure area is mainly distributed in the rear of the turbine and the intermediate section of the deflector hood, which forms a pressure difference between the inlet section and the intermediate section to produce suction, and the deflector hood has a more obvious accelerating effect on the flow field around the hydraulic turbine.

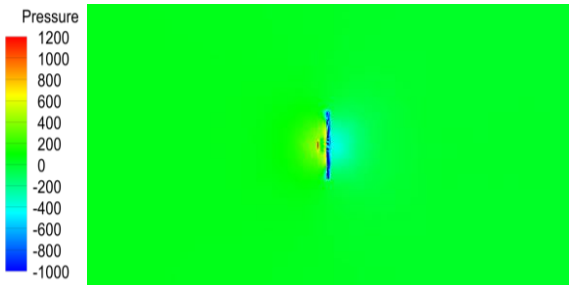

α=0°，β=0°

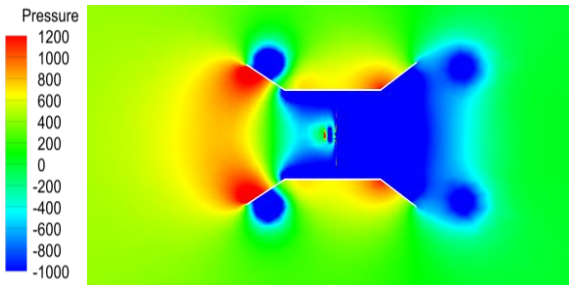

α=29°，β=40°

Fig. 8 Pressure cloud diagram

The velocity streamlines in the vicinity of the turbine without and with the deflector are shown in Fig. 9 for comparison:

(1) When the incoming flow passes through the turbine without the installation of the deflector, the sea current at the blades, especially at the tip of the blades, cannot be supplemented and the pressure is lowered, and the sea current is pressed to flow towards the tip of the blades. At this time, the upward sea current in the wall viscous force and the upper and lower pressure difference force, the sea current speed decreases more; when the sea current over the blade to reach the back of the turbine, it will be in the front and rear of the

reverse pressure difference force under the action of the backflow vortex, so that the sea current flow line disorders.

(2) When the deflector is installed, it plays a guiding role for the sea currents flowing through its vicinity, and the overall flow line is more gentle, thus reducing the friction and resistance loss of the sea currents to the turbine blades, and improving the energy-acquisition efficiency of the tuibine.

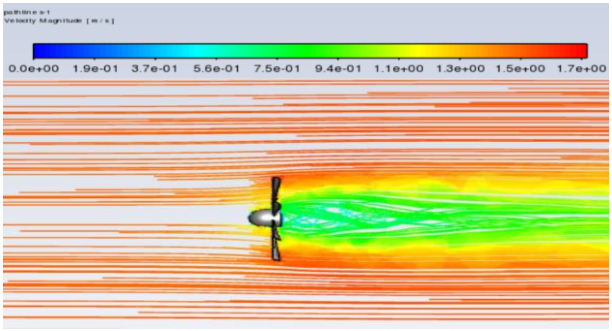

α=0°, β=0°

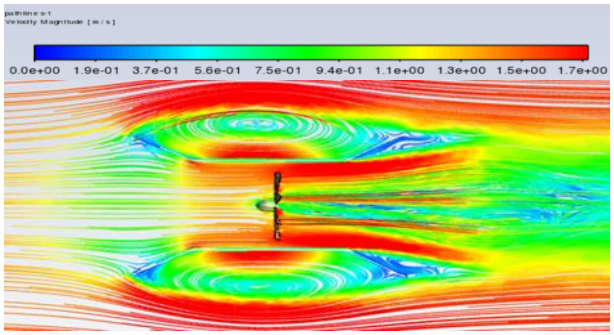

α=29°, β=40°

Fig. 9 Flow diagram

6. Conclusion

In this paper, a three-dimensional model of the horizontal axis tidal current energy turbine and the deflector cover is established, and numerical simulation analyses are carried out based on the CFD method for the deflector cover with different inlet section and outlet section flare angles, and the main conclusions are as follows:

(1) The installation of a linear deflector on the turbine can improve the energy efficiency of the turbine. Among them, changing the angle of the inlet section contributes more to the energy-acquisition efficiency of the hydraulic turbine than changing the angle of the outlet section. When the angle of the inlet section is 29° and the angle of the outlet section is 40°, the energy-acquisition efficiency of the turbine reaches a maximum of 43.81%, which is nearly three times higher than that of 11.15% without the deflector.

(2) After the installation of the deflector, the high-pressure zone formed in the inlet section creates a large pressure difference with the low-pressure zone in the intermediate section, and the velocity gradient of the flow field near the turbine increases, thus increasing the rotational speed of the turbine and improving the energy-acquisition efficiency of the turbine.

(3) The deflector can effectively guide the flow of fluid mass in the vicinity of the turbine, resulting in a smoother flow line and less flow energy loss, thus further improving the energy-acquisition efficiency of the turbine.

References

Liu Yanjun, Jia Rui, Zhang Jian. (2016), Research status a nd development prospects of wave energy power generatio n technology. Journal of Ocean Technology, 35(5), pp.100-104.

Song Ke, Wang Wenquan, Yan Yan. (2019), Research o n hydrodynamic performance of new combined tubular tur bine. Journal of Hydroelectric Engineering,38(06), pp.113-1 20.

Liu Heng, WANG Wenquan, Yan Yan. (2017), Researc h on hydrodynamic and structural performance of horizont al axis ocean current turbine under variable pitch angle. Jo urnal of Drainage and Irrigation Machinery Engineering,35 (05), pp.393-397.

KHAN M J, BHUYAN G, IQBAL M T, et al.(2009), Hy drokinetic energy conversion systems and assessment of ho rizontal and vertical axis turbines for river and tidal applic ations: A technology status review. Applied Energy, 86(10), pp. 1823-1835.

PANWAR N L, KAUSHIK S C, KOTHARI S.(2011), Ro le of renewable energy sources in environmental protectio n: A review. Renewable and Sustainable Energy Reviews, 15(3) pp. 1513-1524.

LUND H.(2007), Renewable energy strategies for sustainab le development. Energy, 32(6) pp. 912-919.

Zhang Lin, Li Xing Zhong, Geng Jing, et al.(2013), Resea rch Status of Tidal Energy in 2013 [J]. Advances in New and Renewable Energy, 1(01) , pp.53-68.

Cui Baoyu, Si Xiancai, Yuan Peng, et al. (2022), Numeric al study on the influence of solidity on the performance of a ducted turbine [J]. Acta Energiae Solaris Sinica, 43(02), pp. 69-74.

Lan Yamei, Zhang Tingting, Wang Shiming, et al. (2020), Research on the influence of deflector structural paramets on the performance of horizontal axis turbines [J]. Water

Power, 46(10) pp. 88-91,121.

Wang Shujie, Xu Shiqiang, Yuan Peng, et al. (2020), Res earch on hydrodynamic characteristics of the duct of axial flow tidal energy power generation device [J]. Acta Energi ae Solaris Sinica, 35(06) pp. 1098-1104.

SONG K, WANG W-Q, YAN Y. (2019), Numerical and experimental analysis of a diffuser-augmented micro-hydro turbine. Ocean Engineering, 171 pp. 590-602.

LI Y, PAIK K-J, XING T, et al. (2012), Dynamic overset CFD simulations of wind turbine aerodynamics. Renewabl e Energy, 37(1) pp. 285-298.

Liu Nansheng, Lu Xiyun, ZHUANG L X. (2005), Effec ts of rotation on near-wall turbulence characteristics and fl ow field structure. Science in China Series G: Physics, Me chanics & Astronomy, (01) pp. 87-108.

WANG F J.(2016), Research progress on computational m odels of rotating turbulence in fluid machinery [J]. Transac tions of the Chinese Society for Agricultural Machinery, 4 7(02) pp. 1-14.

LUO Ruidong. (2020), Design and hydrodynamic analysis of a suspended horizontal axis tidal turbine and its duct.

BAHAJ A S, BATTEN W M J, MCCANN G. (2016), E xperimental verifications of numerical predictions for the h ydrodynamic performance of horizontal axis marine current turbines. Renewable Energy, 32(15) pp. 2479-2490.

KERDOUSS F, BANNARI A, PROULX P. (2016), CFD modeling of gas dispersion and bubble size in a double tu rbine stirred tank. Chemical Engineering Science, 61(10) p p. 3313-3322.

Received **15 May 2024**

1st Revised **20 June 2024**

Accepted **27 June 2024**